

RESEARCH ARTICLE | MARCH 01 2019

Estimation of wind pressure acting on the new palm house in Gdansk

Jacek Chróścielewski; Mikołaj Miśkiewicz; Bartosz Sobczyk ; Krzysztof Wilde



AIP Conf. Proc. 2078, 020023 (2019)

<https://doi.org/10.1063/1.5092026>



View
Online



Export
Citation

CrossMark

AIP Advances

Why Publish With Us?

-  **25 DAYS**
average time to 1st decision
-  **740+ DOWNLOADS**
average per article
-  **INCLUSIVE**
scope

[Learn More](#)

Estimation of Wind Pressure Acting on The New Palm House in Gdansk

Jacek Chróścielewski^{1, b)} Mikołaj Miśkiewicz^{1, c)}
Bartosz Sobczyk^{1, a)} and Krzysztof Wilde^{1, d)}

¹*Gdańsk University of Technology, Faculty of Civil and Environmental Engineering
G. Narutowicza Street 11/12, 80-233 Gdańsk.*

^{a)}Corresponding author: bartosz.sobczyk@pg.edu.pl

^{b)}jacek.chroscielewski@pg.edu.pl

^{c)}mikolaj.miskiewicz@pg.edu.pl

^{d)}krzysztof.wilde@pg.edu.pl

Abstract. This paper deals with the problem of numerical simulations of wind loads acting on a Palm House with complex geometry. Flow simulations with aid of computational fluid dynamics procedures have been performed to check if the pressure distributions for the structure are greater than those calculated using the standard design codes with assumption that the Palm House horizontal cross sections are described by smooth cylinders.

INTRODUCTION AND AIM OF THE PAPER

It is quite popular in large municipalities to build structures with unusual shapes to emphasize the status and character of some institutions, museums, offices, etc. and to attract or impress citizens and tourists. The new Palm House in Gdansk is an example of such a building.

The idea to replace the old building with a new one, in order to protect the palm tree being approximately 150 years old today. The problem became significant when the total height of the tree became close to the height of the old building and the palm levees started to break glass windows of the roof. In consequence, some concepts of the shape of the new building emerged and finally the design process was launched in 2016. The building is currently under construction, as it is shown in Fig. 1.



FIGURE 1. The Palm house under construction, private Authors' photos taken on October 2018

The new Palm House is a space frame made of steel. It is built of twenty columns, having different angles of vertical inclination and square hollow sections (SHS) with different dimensions changing in the height direction of the house. The columns are tied with transverse beams and additional bracings. The aforesaid elements form a quasi-cylindrical structure with spherical roof. The whole steel structure is covered with a glass facade. The total height of the house is 24 m, whereas its width is 16 m. Since the columns are inclined the structure has different cross sections having sprocket type shapes. The visualization of the of the Palm House geometry, with locations of some representative sections of the glass façade contour, within the quasi cylindrical part, is shown in Fig 2. The sections A-A, B-B and C-C are shown in Fig. 3.

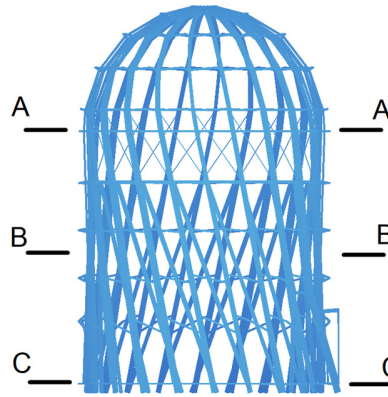


FIGURE 2. The visualization of the Palm House geometry with location of the representative sections

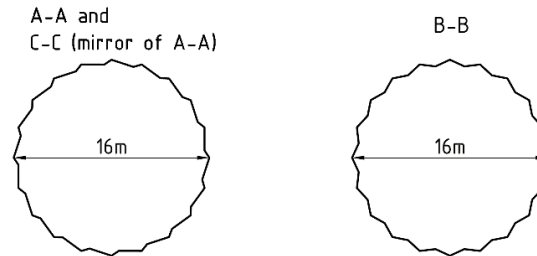


FIGURE 3. Cross sections of the house structure

Two types of edges: short and long can be distinguished for the sprocket sections A-A and C-C. The short edge, located at the bottom of the house (section C-C) is swept in the direction of the inclined column and simultaneously its length is growing to become a long one at section A-A. Similarly the long edge at C-C becomes a short one at A-A. Therefore A-A and C-C sections have the same configuration of sprocket and one is a reflection of the other. At the mid-height (B-B) the edges have equal length. Thus, the surface to be covered with glass facade is created by such a sweep of edges.

As shown in previous paragraphs, the palm house has a complex geometrical form. However, if it is intended to use design codes, as [1] its side surface needs to be simplified and e.g. treated as a smooth cylinder in order to estimate wind pressure acting on the facade. This seems to be a too far-reaching assumption and some doubts arise. The convex and concave vertices of the cross section can disturb the air flow. Therefore, the pressures may increase locally in the corners, as opposed to a smooth distribution of wind pressure for the cylinder. All the directions of wind acting on the cylinder result in the same pressure distribution patterns, however it seems that for the Palm House this does not have to be true. For example it is expected that the wind pressure distributions resulting from wind hitting the convex corner will be not the same as the ones induced by the wind hitting the concave corner. Finally it is not clear whether there will be any significant change in the intensity of wind action. All the aforesaid problems are considered within this paper.

ESTIMATION OF WIND PRESSURE

Wind pressure for a cylinder

Estimation of wind pressure distribution for a cylinder is made first to get some reference values for further considerations. Some typical procedures are available in the design codes, see e.g. [1] for the purpose of wind load estimation. Hence, the pressure is calculated assuming that a pure cylinder has a diameter of 16 m (the same as the width of the Palm House). The coordinate above the ground for the wind velocity calculation is set to 17 m, which corresponds with the height of the quasi cylindrical part of the structure and therefore enables to take into account maximum velocity that can occur around this part of structure. The velocity is 38.15 m/s and the Reynolds number for the flow is $Re \sim 4 \times 10^7$. According to [1] and assuming the terrain category to be III, because of the surrounding of the Palm House, the pressure distributions shown in Fig. 4 are determined.

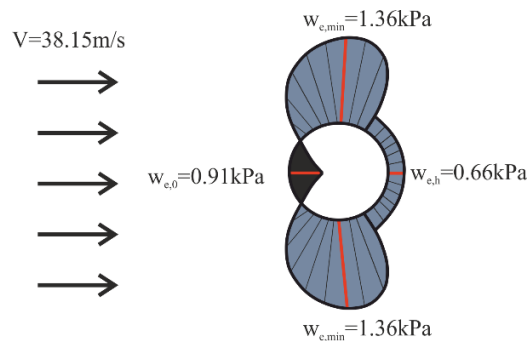


FIGURE 4. Distribution of wind pressure (colored in black) and suction (grey color) for the cylinder

It is worth noticing, that the distribution from [1] is symmetric and thus it is tacitly assumed in [1] that the dynamic effects of wind flow are neglected in the design which is a simplification and may lead to load under estimation.

Additionally, calculations of wind flow around a circular cylinder are made in order to check whether the problem can be properly described using CFD in the considered flow regime. The mean drag coefficient obtained in the course of the analysis equals 0.25 and it corresponds well with the reference value 0.3 available in the code [1]. The drag coefficient is calculated basing on the distribution of pressure on the cylinder wall. Therefore, it can be concluded that the pressure is accurately estimated. Also the Strouhal number (St) is compared. It is ~ 0.4 in the current CFD simulation. Unfortunately the reference values for the St are given only up to $Re \sim 1 \times 10^7$ (refer for example to [2]) and $St(Re \sim 1 \times 10^7) = 0.3$. However, it can be observed that the St tends to increase in the range between $Re \sim 5 \times 10^6$ and $Re \sim 1 \times 10^7$. If the function $St(Re)$ is extrapolated, then St close to 0.35 is obtained for $Re \sim 4 \times 10^7$. Thus, the calculated St corresponds with the reference one. Basing on the comparison of the drag coefficient and St number it can be concluded that the CFD is suitable to describe the flow in the analyzed regime.

Wind Pressure For The Palm House

It is a common practice to analyze influence of wind flow on structures by means of computational fluid dynamics (CFD) and finite volume method (FVM), refer to [3] or [4–10] for some recent studies. The same approach is used hereafter.

It is obvious that the wind effects on the Palm House are three dimensional (3D) and CFD simulations should be 3D as well. Nevertheless, as the problem is addressed to engineers, some simple and quick methods of wind load estimations have to be employed.

Therefore, we analyze the wind pressure/suction distributions for the representative cross sections A-A, B-B and C-C, as 2D estimations, aiming to create an envelope of most extreme conditions for the whole 3D structure. The simulations of the entire spherical dome have been therefore omitted.

Since the cross sections are located at different heights, the different wind velocities should be considered as initial conditions. The Reynolds numbers for wind velocities that can occur at different heights classify all the flows to the supercritical regime. Thus, in order to reduce the number of analyzes to be executed, all the cross-sections are



subjected to extreme wind velocity that can appear at the level ($z = 17$ m) where the quasi cylindrical part and the dome are connected. Then the pressures are scaled to adjust them to the wind velocity at certain level above the ground.

It is expected that for this class of flows ($Re \sim 4 \times 10^7$) turbulences and flow perturbations will occur on the leeward side of the sprocket sections and therefore all the calculations are transient. This enables to capture the influence of the flow change on the pressure/suction distributions on the side of the sprocket walls.

CFD Simulations

Four 2D domains have been created to analyze the wind flow, study possible wind directions and configurations of the sprocket sections. This domains, therefore cover the cases of wind attacking the convex and concave corner of A-A/C-C and B-B sections. The global dimensions of the domains are shown in Fig. 5. They are chosen in such a way that they do not affect the estimations. The domains elongate in the leeward direction and are shorter on the windward side. The difference between them regards to the aforesaid configuration of sprocket sections and wind directions.

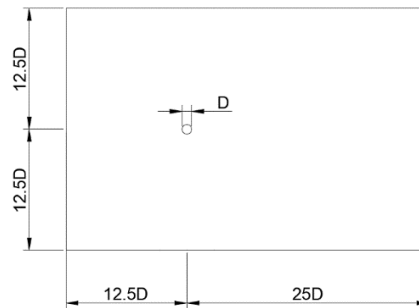


FIGURE 5. The 2D computational domain size, $D=16$ m.

The code [1] is used to determine the initial conditions of the wind in the area of Palm House. The same extreme wind velocity 38.15 m/s, as for the estimation of pressure/suction of the cylinder, is used and assigned at the inlet of the domain as a boundary condition. Pressure conditions, $p = 0$ are applied to the outlet of domain. The sprocket sections are treated as no-slip walls. The boundary conditions are depicted in Fig. 6.

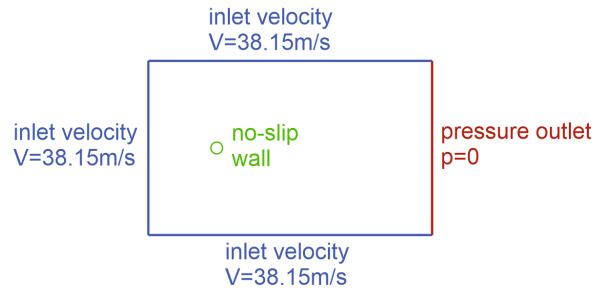
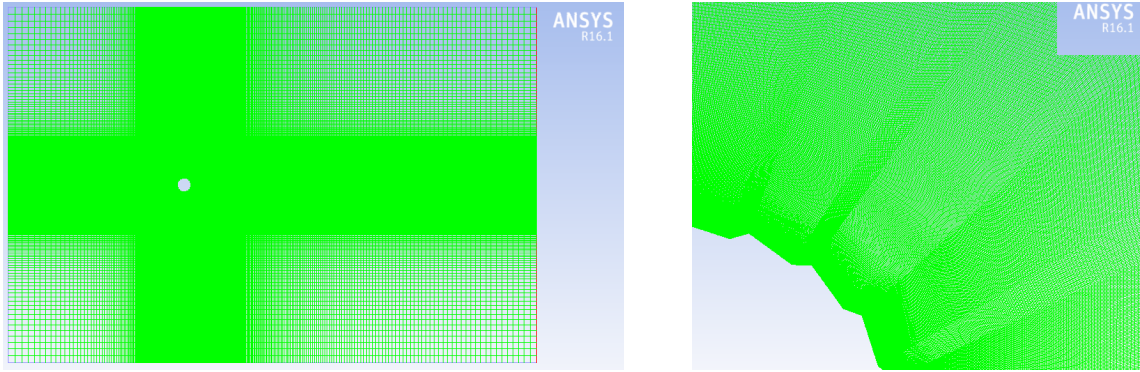


FIGURE 6. Boundary conditions of the domain.

The ANSYS Fluent 16.1 FVM code is used to solve the equations describing the wind flow. It is expected that for this flow regime ($Re \sim 4 \times 10^7$) turbulences may occur and the flow will be unsteady, therefore $k-\epsilon$ model is incorporated with the equations of the problem.

The 2D domain is divided into cells in such a way that the mesh is very fine in the surrounding of the sprockets. The mesh coarsens close to the domain borders, as shown in Fig. 7. The mesh has been created with respect to the turbulence model requirements. The total number of nodes for each of the considered domain is approximately 1 million.



(a)

(b)

FIGURE 7. Visualizations of the mesh: a) view of the whole domain, b) zoom of the sprocket wall surrounding

Some selected results of the calculations are shown below. Fig. 8 and 9 depict the contours of the velocity magnitude for the A-A and B-B section sprocket, respectively, when the flow is fully developed and clearly unsteady.

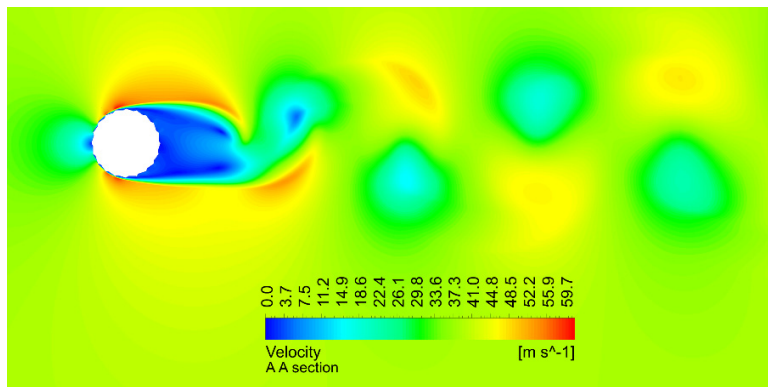


FIGURE 8. Velocity magnitude contours for A-A section

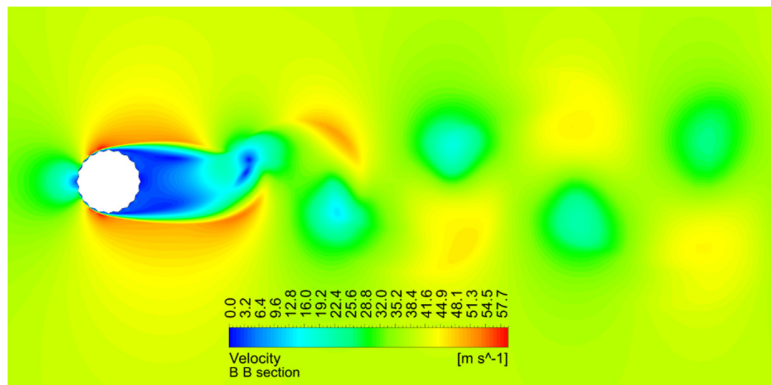


FIGURE 9. Velocity contours for B-B section

The wall pressure/suction distributions for the B-B section for wind attacking the concave corner at the moment when extreme lift acts in the downward direction is presented in Fig. 10. Similarly, the distributions for the A-A/C-C sections are presented for: the wind attacking the concave corner and extreme upward lift in Fig. 11; the wind attacking the convex corner and extreme downward lift in Fig. 12. To keep the clarity of Fig. 10 – Fig. 12 for each single presented case the distributions are divided into two schemes and thus some empty edges are always left.

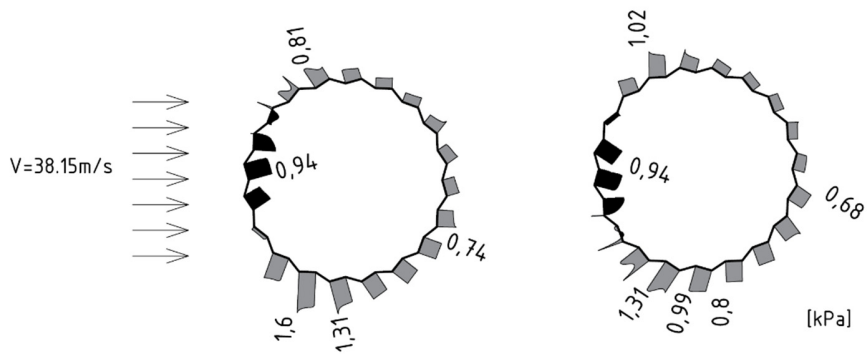


FIGURE 10. Distributions of wind action for the B-B section, the wind attacks the concave corner, results shown for the extreme downward lift, pressure colored in black, suction in grey

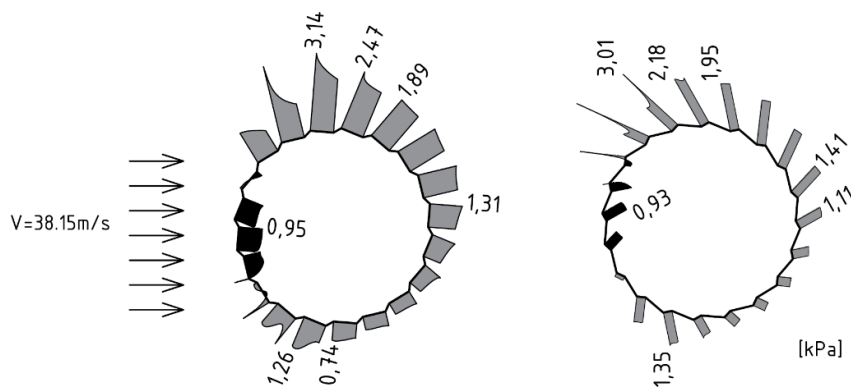


FIGURE 11. Distributions of wind action for the A-A/C-C section, the wind attacking the concave corner, extreme upward lift, pressure colored in black, suction in grey

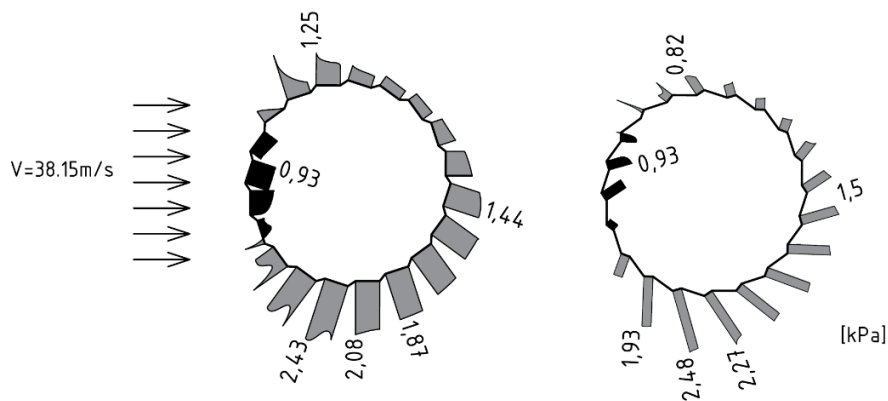


FIGURE 12. Distributions of wind action for the A-A/C-C section, the wind attacking the convex corner, extreme downward lift, pressure colored in black, suction in grey

The distribution patterns for the sprocket sections (Fig. 10 – Fig.12), compared to the one for a cylinder (refer to Fig. 4) are significantly different, they are not as smooth as for the cylinder. The effects of unsteady flow are clearly revealed (asymmetry of the pressure/suction regarding wind direction). What is more, obtained values of pressure/suction for the sprocket sections are significantly greater than for the cylinder. On the one hand, some strongly local effects can be observed at the sprocket corners, resulting in the values of suction close to 3.2 kPa.

Globally the suction on the sprocket cross-section equals approximately 2.5 kPa while the extreme suction for the smooth cylinder, in the same condition, is only 1.36 kPa.

FINAL REMARKS

The CFD analysis of the selected sections of the new Palm House in Gdańsk reveals that the wind pressures/suctions distribution on the facade of the house are significantly greater (even ~1.8 times) than the ones calculated assuming that the facade is treated as a cylinder. What is more due to the effects of unsteady flow the pressure distribution patterns for the sprocket house sections, compared to the ones for the cylinder, are different as well. Therefore, a simplification of its shape could lead to underestimation of the wind load effects that could result in damage or even collapse of the structure.

REFERENCES

1. PN-EN 1991-1-4:2008: Eurocode 1: Actions on structures - Part 1-4: General actions – Wind actions.
2. M. A. Zahari and S. S. Dol, *Journal of Applied Sciences* **15**, 783-791 (2015).
3. H. Versteeg and W. Malalasekera, *An Introduction to Computational Fluid Dynamics: The Finite Volume Method (2nd Edition)* (Longman Group Ltd, Burnt Mill, Harlow, 1995).
4. I. Kavrakov and G. Morgenthal, *J. Fluids Struct.* **82**, 59-85 (2018).
5. B. Dose, H. Rahimi, I. erráz, B. Stoevesandt, and J. Peinke, *Renew. Energy* **129**, 591-605 (2018).
6. S. Liu, W. Pan, X. Zhao, H. Zhang, X. Cheng, Z. Long, and Q. Chen, *Build. Environ.* **140**, 1-10 (2018).
7. P. Omenzetter, K. Wilde, Y. Fujino. *J. Eng. Mech.-ASCE* **128**, 264-279 (2002).
8. B. Sobczyk, J. Chróścielewski, W. Witkowski, *Biuletyn WAT LXIV*, 91-101 (2015).
9. A. Padewska, P. Szczepaniak, A. Wawrzynek, *Computer Assisted Methods in Engineering and Science*, **21**, 151-167 (2014).
10. F. Toja-Silva, T. Kono, C. Peralta, O. Lopez-Garcia, and J. Chen, *J. Wind Eng. Ind. Aerodyn.* **180**, 66-87 (2018).